Original Research Communication

v-Ha-Ras Overexpression Induces Superoxide Production and Alters Levels of Primary Antioxidant Enzymes

JI-QIN YANG, SHIJUN LI, YUANHUI HUANG, HANNAH J. ZHANG,
FREDERICK E. DOMANN, GARRY R. BUETTNER, and LARRY W. OBERLEY

ABSTRACT

Reactive oxygen species have been shown to play important roles in v-Ha-Ras mitogenic signaling. We hypothesized that v-Ha-Ras overexpression would induce superoxide production, and therefore modify expression of the primary antioxidant enzyme system. We have demonstrated that immortal rat kidney epithelial cells stably transduced with constitutively active *v-Ha-ras* produced significantly larger amounts of superoxide radical than wildtype or vector-transfected control cells. The levels of the primary antioxidant enzymes copper- and zinc-containing superoxide dismutase, manganese-containing superoxide dismutase, catalase, and glutathione peroxidase were increased in the superoxide-overproducing cells. DNA-binding activities of the transcription factors activator protein-1, activator protein-2, and nuclear factor-κB were all enhanced in the superoxide-overproducing cells. These *v-Ha-ras* transduced cells also had a shortened cell doubling time and higher plating efficiency, and displayed greater constitutive levels of phosphorylated mitogen-activated protein kinases. These data demonstrate that v-Ha-Ras overexpression increases superoxide production and this apparently affects a wide variety of cell signaling and redox systems. Antioxid. Redox Signal. 3, 697–709.

INTRODUCTION

ONCOGENIC *RAS* is one of the most studied genes in cancer; ~30% of all human tumors contain mutated versions of Ras protein (4). The Ras family of proto-oncogenes encode 21-kDa membrane-anchored, GTP-binding proteins that transduce mitogenic signals from the tyrosine-kinase receptors (23). Harvey virus v-Ha-Ras, which is mutated in the 12th and 59th amino acids, is a kind of dominant activated Ras (16).

Reactive oxygen species (ROS), including superoxide, hydrogen peroxide, and hydroxyl radical, are constantly produced by metabolic reactions in the human body (5, 18). Three types of large-molecular-weight primary anti-oxidant enzymes (20)—the superoxide dismutases (SODs), catalases (CATs), and peroxidases [such as glutathione peroxidase (GPx) and thioredoxin peroxidase]—mainly control the intracellular level of ROS. The SODs convert superoxide into hydrogen peroxide, whereas the CATs, GPxs, and thioredoxin peroxidases convert hydrogen peroxide to harmless water. The overproduction of superoxide or hydrogen peroxide will influence activities of important regulatory proteins. In various cells, the activation of mitogen-activated protein kinase (MAPK) by the stimulation of growth factors is dependent on the production of ROS (7, 14, 15, 30). MAPKs such as p44/42 MAPK, p38 MAPK, and c-Jun N-terminal kinase (JNK) MAPK are activated through phos-

phorylation; their activation leads, in turn, to phosphorylation and activation of transcription factors (17, 25, 27). The transcription factors nuclear factor-κB (NF-κB), activator protein-1 (AP-1), and AP-2 (9) can bind to specific DNA sequences and induce their gene expression, including some of the genes involved in oxidative stress and mitogenic signaling.

Generally, cancer cells have low levels of manganese-containing SOD (MnSOD) and copper- and zinc-containing SOD (CuZnSOD) when compared with their normal cell counterparts (19, 20); this implies that superoxide has a role in the cancer cell phenotype. Recent studies have connected Ras-induced mitogenesis and superoxide production (11); increased superoxide production in cancer may be a general phenomenon because tumor cells have such a high rate of *ras* gene mutation. We have recently shown in a nonmalignant, but immortal, human keratinocyte cell line that *ras*-transduced cells also had increased levels of superoxide radicals (32). In the present work, we have extended our studies to immortal rat kidney epithelial cells to investigate further the effects of the *v-Ha-ras* transfection on superoxide production and mitogenic signaling. Using a *v-Ha-ras* expression vector encoding a dominant activated Ras to transfect immortal rat kidney epithelial cells, we demonstrated that *v-Ha-ras* overexpression (a) mediated an increase in cellular superoxide production, (b) altered primary antioxidant enzyme levels, and (c) shortened cell population doubling time and increased plating efficiency. In addition, p44/p42 and p38 MAPK were activated in Ras transduced cells, as were the DNA-binding activities of AP-1, AP-2, and NF-κB. Our findings suggest that Ras might mediate mitogenic signaling through altering of superoxide production. This work is the first to report changes in primary antioxidant enzyme levels after *ras* transfection.

MATERIALS AND METHODS

Cell culture

The immortal, nonmalignant rat kidney epithelial cell (REC) line, NRK52E, was a gift from Dr. Michael Robbins (Free Radical and Radiation Biology Program, The University of Iowa). It was originally obtained from ATCC: line CRL-1571. Cells were maintained in high-glucose Dulbecco's modified Eagle's medium containing 5% bovine calf serum, 2 mM L-glutamine, and 0.1 mM nonessential amino acids at 37°C in 5% CO_2. Cells were fed three times a week. Cells were given to us at passage 6 after procurement from ATCC. After transfection and selection as described below, the cells were at passage 10. The cells used in our studies were between 10th and 30th passages.

v-Ha-ras cDNA transfer

The *v-Ha-ras* encoding pZIPNeoSV(X)1 plasmid was used as the vector to generate stably transfected cell lines. This plasmid was kindly provided by Dr. Richard C. Milligan (Department of Biology and Center for Cancer Research, Massachusetts Institute of Technology, Cambridge, MA, U.S.A.). The *v-Ha-ras* cDNA is driven by a viral LTR promoter (3). REC cells (1×10^6) were seeded in six-well plates and allowed to grow for 24 h. The medium was removed, and the cells were transfected with 2 μg of the *v-Ha-ras*-pZIPNeoSV(X)1 construct and 10 μl of Lipofectamine (Life Technologies, Gaithersburg, MD, U.S.A.) as vehicle per dish. Selection for neomycin-resistant clones was performed with G418 (400 μg/ml), and individual colonies were obtained. G418 was removed 3 days before an experiment. The clone designated as Neo was also transfected with *v-Ha-ras*-pZIPNeoSV(X)1, but did not express *v-Ha-ras*.

Western blotting analysis

Cells were harvested and lysed by sonication, and then proteins (concentrations quantified using Bio-Rad protein assay kit) separated by 12.5% sodium dodecyl sulfate–polyacrylamide gel electrophoresis (SDS-PAGE). The proteins were electrotransferred to nitrocellulose sheets. After blocking in 5% milk for 30 min, the sheets were washed and treated with antibody to pan-Ha-Ras (purchased from Oncogene Science, Cambridge, MA, U.S.A.; 1:1,000), antisera to MnSOD (1:1,000), CuZnSOD (1:1,000), CAT (1:1,000), antibody to phosphorylated-

p44/p42 MAPK (1:1,000), phosphorylated-p38 MAPK (1:1,000), or phosphorylated-JNK (1:1,000) (New England Biolabs Inc., Beverly, MA, U.S.A.) for 30 min. Polyclonal rabbit antibodies to human MnSOD, CuZnSOD, and CAT were prepared and characterized in our laboratory (21). The blot was incubated with horseradish peroxidase-conjugated goat anti-rabbit or anti-mouse IgG (Sigma Chemical Co., St. Louis, MO, U.S.A.; 1:10,000) for 1 h at room temperature. The washed blot was then treated with enhanced chemiluminescence western blot detection solution (Amersham Life Science, Buckinghamshire, U.K.) and exposed to x-ray film.

Northern blotting analysis

Total RNA was isolated by the acid guanidinium thiocyanate–phenol–chloroform extraction method and then quantified by microspectrometry. RNA (18 μg) was separated on a 1.5% agarose formaldehyde gel. RNA was transferred to a nylon membrane; the membrane was then preincubated with hybridization buffer [50% formamide, 5$\times$ saline–sodium citrate buffer (SSC), 10% dextran sulfate, 1$\times$ Denhardt's buffer, 1% SDS, and 150 μg/ml denatured salmon sperm DNA] and hybridized to a ^{32}P-labeled probe made from v-Ha-ras cDNA. Following hybridization, the membrane was washed in 2$\times$ SSC, 0.5% SDS solution twice for 15 min each at room temperature and then washed in 0.1$\times$ SSC, 0.5% SDS solution twice for 15 min each at 65°C. The membrane was wrapped in plastic wrap and exposed to x-ray film (Kodak, Rochester, NY, U.S.A.) at −80°C overnight. 18S RNA was used to normalize the amount of RNA loading.

SOD-inhibitable cytochrome c assay for superoxide production

The production of superoxide was measured by its reduction of cytochrome c (2). Cells were cultured in six-well plates. The medium was then removed and cells washed twice in Krebs–Ringer buffer. Cytochrome c (100 μM) in Krebs–Ringer buffer with CAT (200 U/ml) was added to the wells; samples were removed after 1 h of incubation at 37°C in 5% CO_2. The spectrum of each sample was then taken between 400 and 600 nm. Superoxide production was determined by measuring the peak height at 550 nm over the baseline between 530 and 560 nm. Cytochrome c can be reduced by the superoxide radical anion ($O_2^{\cdot-}$) from cyt c (Fe^{3+}) to cyt c (Fe^{2+}), with a rate constant $k = 1.5 \times 10^5\ M^{-1}\ s^{-1}$ (pH 7–9.3), and extinction coefficients of cyt c (Fe^{2+})$\epsilon_{m550} = 2.99 \times 10^4\ M^{-1}$ cm^{-1} and cyt c (Fe^{3+}) $\epsilon_{m550} = 0.89 \times 10^4\ M^{-1}$ cm^{-1} (6).

SOD, CAT, and GPx activity gel assays

SOD, CAT, and GPx activities were measured using native gel activity stains. An 8% polyacrylamide running gel and 5% stacking gel were used to separate the proteins. For the SOD activity stain (1), the gel was stained with 2.43 mM nitro blue tetrazolium solution for 20 min and then 28 μM riboflavin with 28 mM N,N,N',N'-tetramethylethylenediamine (TEMED) for 15 min. The gel was placed in distilled water and illuminated under a bright fluorescent light. Achromatic bands indicated the presence of SOD. For the CAT activity stain (28), the gel was first rinsed three times with distilled water, then incubated in 0.003% hydrogen peroxide for 10 min. The gel was then stained with 2% ferric chloride and 2% potassium ferricyanide; when achromatic bands began to form, the stain was poured off and the gels were rinsed extensively with distilled water. Achromatic bands demonstrated the presence of CAT activity. A similar procedure was used for GPx activity (28). Gels were first soaked in three changes of reduced glutathione for a total of 45 minutes, then soaked in 0.008% cumene hydroperoxide plus reduced glutathione for 10 min. The gels were rinsed twice with distilled water and then stained with ferric chloride and potassium ferricyanide as described above.

Plating efficiency

Cells were plated in triplicate into 60-mm dishes in complete medium The number of cells plated was 100 or 500. The dishes were maintained in the incubator for 14 days to allow colony formation. Colonies were then fixed and stained with 0.1% crystal violet and 2.1% citric acid, and those colonies containing >50 cells were scored.

Cell population doubling time assay

Cells (2×10^4) were plated in 1.5 ml of complete medium in 24-well plates; the medium was changed every 4 days. Cells were trypsinized and then counted on alternate days for 2 weeks using a hemocytometer. Cell population doubling time (DT) in hours was determined using the following equation (13):

$$DT \text{ (hours)} = 0.693 \, (t - t_0)/\ln (N_t/N_0)$$

where t_0 is time at which exponential growth began, t is time in hours, N_t is cell number at time t, and N_0 is initial cell number.

Gel mobility shift assay

Nuclear protein was extracted by the following procedure. Cells were collected when 80% confluent and rinsed with phosphate-buffered saline buffer. Cells were then harvested by scraping in ice-cold buffer A (10 m*M* HEPES, 1.5 m*M* MgCl$_2$, 10 m*M* KCl) and incubated on ice for 20 min. The cells were lysed with a Dounce homogenizer (Kontes, Vineland, NJ, U.S.A.), and the nuclei were pelleted by centrifuging twice at 1,400*g* for 30 s at 4°C with subsequent removal of supernatant. The nuclear pellets were resuspended in ice-cold buffer C (20 m*M* HEPES, 25% glycerol, 0.42 *M* NaCl, 1.5 m*M* MgCl$_2$, 0.2 m*M* EDTA, 0.5 m*M* phenylmethylsulfonyl fluoride) and placed on ice for 15 min. The suspensions were centrifuged (14,000*g* for 10–15 min), and the supernatants were removed and diluted with ice-cold buffer D (20 m*M* HEPES, 20% glycerol, 0.1 *M* KCl, 0.2 m*M* EDTA, 0.5 m*M* phenylmethylsulfonyl fluoride). The protein concentrations were determined, and nuclear protein extracts were stored at −80°C.

DNA binding reactions were carried out with 1.5 μg of extracted nuclear protein and double-stranded synthetic oligodeoxynucleotide encompassing an AP-1 consensus sequence 5′-agcttgTGACTCAccgtag-3′, AP-2 consensus sequence 5′-agctcaaGCCCGCGGGCtctctag-3′, or NF-κB consensus sequence 5′-agctga-GGGGACTTTCCctag-3′. Probes were ^{32}P-labeled using Klenow DNA polymerase and [α-^{32}P]dCTP. Nuclear protein extracts (1.5 μg) were incubated with ^{32}P-labeled DNA probes in the presence of 1 μg of poly(dIdC) (Pharmacia Biotech Inc., Piscataway, NJ, U.S.A.) and 1× gel shift buffer (10 m*M* Tris, pH 7.5, 50 m*M* NaCl, 1 m*M* MgCl$_2$, 0.5 m*M* EDTA, 0.5 m*M* dithiothreitol, 4% glycerol) at room temperature for 20 min. The bound DNA–protein complexes were separated from free probe by gel electrophoresis in 5% native polyacrylamide gels in 1× TBE (90 m*M* Tris-borate, 2 m*M* EDTA). Electrophoresis was conducted at a constant current of 20 mA for 1 h. The gel was wrapped in a plastic wrap and exposed to x-ray film overnight at −80°C. AP-1 DNA-binding specificity was determined by competition experiments. Nuclear protein extracts (1.5 μg) were preincubated with 1 μg of poly(dIdC), 1× gel shift buffer, and a 10- or 100-fold excess of unlabeled AP-1, AP-2, or NF-κB oligonucleotides for 15 min at room temperature before the addition of the labeled probe. For supershift assays, nuclear protein extracts (1.5 μg) were preincubated with 2 μg of anti-c-Jun/AP-1, anti-AP-2α, or anti-p50 (NF-κB) antibodies (Santa Cruz Biotechnology, Santa Cruz, CA, U.S.A.) for 30 min at room temperature and then incubated with ^{32}P-labeled probes.

Statistical analysis

Statistical analysis was performed using SYSTAT (Systat, Evanston, IL, U.S.A.). A single factor analysis of variance, followed by a post-hoc Tukey test, was used to determine statistical differences between means. The null hypothesis was rejected at the 0.05 level of significance. All means were calculated from three experiments, and error bars represent standard deviations (SD). All western blot and activity gel assays were repeated at least twice.

RESULTS

v-Ha-ras protein was overexpressed and mediated superoxide production

REC cells were transfected with *v-Ha-ras* through the retrovirus plasmid pZIPNeo-SV(X)1 construct. Clones were selected and the expression of v-Ha-Ras protein was detected by western blotting. The clones with different increased levels of v-Ha-Ras immunoreactive

protein (W13, U12, and U23) were used for further experiments (Fig. 1A). The northern blot (Fig. 1B) demonstrated two new mRNA bands (4.7 and 6 kb) in W13, U12, and U23, but not in REC or Neo; the new bands were therefore generated from the *v-Ha-ras* expression vector. Because of what has been observed earlier in other cells, the likely explanations for the two new bands are the proviral full-length mRNA and a spliced variant. The intensity of the new bands suggested that *v-Ha-ras* was efficiently transcribed in W13, U12, and U23 cells. The 1-kb mRNA from the endogenous *c-Ha-ras* gene was also found; its intensity was increased in W13, U12, and U23 clones. There are at least two possibilities for this observation besides the RNA loading. One is that *c-Ha-ras* oncogene is up regulated by *v-Ha-ras* overexpression; the other is that some *v-Ha-ras* mRNAs decompose to a 1-kb size. These data suggest that the Ras protein comes from the exogenous plasmid, but does not exclude the possibility that some Ras protein may come from the endogenous gene.

Recent evidence has demonstrated that Ras transformed cells can stimulate cellular superoxide production (11, 22, 29, 32). To test if *v-Ha-ras* transduced REC cells produce more superoxide, we used Fe(III) cytochrome *c* to monitor the amount of superoxide production from the cells. Figure 2A shows that *v-Ha-ras*

transduced cells U12 and U23 generated large amounts of superoxide, up to fivefold more than REC or Neo cells. The addition of exogenous CuZnSOD protein totally inhibited the increased superoxide levels seen in U23 cells (Fig. 2B), which demonstrated that the 550-nm peak was due to superoxide production from the cells.

To test whether v-Ha-Ras protein mediated superoxide production, we treated U23 cells with either lovastatin or α-hydroxyfarnesylphosphonic acid (α-PA), inhibitors of Ras protein farnesylation (26); superoxide production was decreased >50% by each of these inhibitors (Fig. 2B), and statistical analysis showed that the difference was significant ($p < 0.05$). This result demonstrated that Ras mediated the superoxide production from the *v-Ha-ras* transduced cells. We did not see complete inhibition; there may be certain functional Ras proteins formed in spite of the drug treatment.

We then studied the source of superoxide production from the *v-Ha-ras* transfected cells. Neutrophils after stimulation are well known to produce superoxide through an NADPH oxidase system (8); there is evidence showing that other types of cells, including epithelial cells, also have an NADPH oxidase system in their plasma membrane (22, 29, 31, 32). Mitochondria are also an important source of superox-
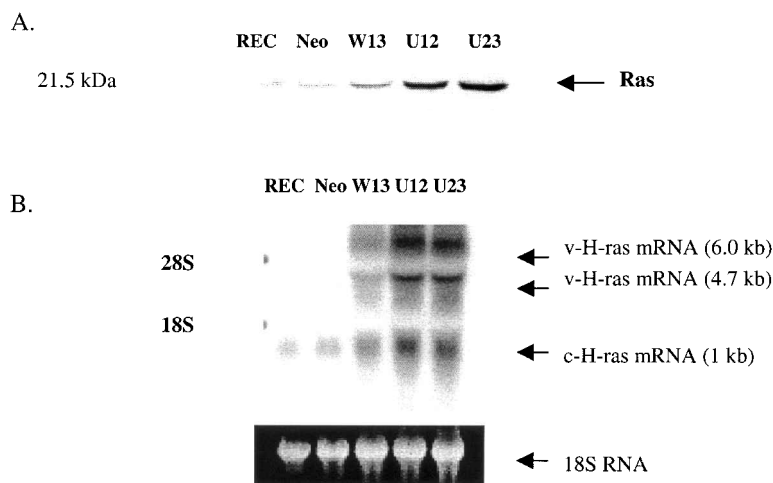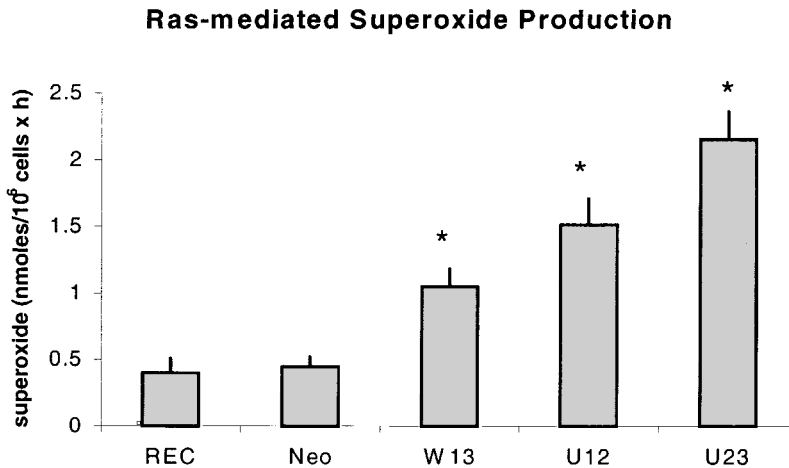

FIG. 1.   v-Ha-Ras was overexpressed in *v-Ha-ras* transduced REC cells. (**A**) Western blotting analysis. Cell lysates (100 μg) were run on 12.5% SDS-PAGE. The proteins were electrotransferred to nitrocellulose sheets and treated with mouse monoclonal antibody to pan-Ras. (**B**) Northern blotting analysis. Total RNA (18 μg) was fractionated on 1.5% agarose gel, transferred onto a nylon membrane, and hybridized with ^{32}P-labeled probe made from human *v-Ha-ras* cDNA. 18S RNA was used to normalize the RNA loading amount.
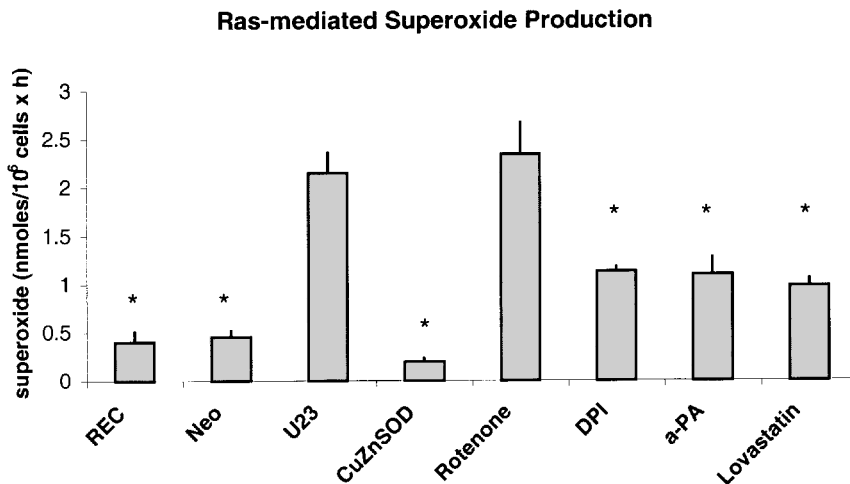
A.

Ras-mediated Superoxide Production

B.

Ras-mediated Superoxide Production

FIG. 2. **Ras mediated superoxide production from the SOD-inhibitable cytochrome c assay.** (**A**) Cells were washed, then incubated with 100 μM cytochrome c in Krebs–Ringer buffer at 37°C, 5% CO_2 for 1 h. Samples were scanned from 400 nm to 600 nm; the 550-nm peak height was measured and adjusted for baseline, and then the amount of superoxide was determined. Means were calculated from three experiments, and error bars represent SD. *Significantly different from REC or Neo at the $p < 0.05$ level. Data indicate that Ras transduced cells had increased levels of superoxide radical. (**B**) U23 cells were further treated with rotenone (50 μM), DPI (100 μM) 2 h, lovastatin (50 μM) 48 h, or α-PA (4 μM) 48 h before measurements, or CuZnSOD protein (200 U/ml final) was added into the cytochrome c solution during the measurement. Cell number was counted after the assay; data were calculated and expressed as the rate of superoxide production per hour (nmol/10^6 cells $\times$ h). Means were calculated from three experiments, and error bars represent SD. *Significantly different from U23 at the $p < 0.05$ level. The data show that CuZnSOD protein, DPI, α-PA, and lovastatin all inhibited superoxide levels.

ide; it is estimated in respiring cells that at least 1–3% of total respiration is used to generate superoxide and hydrogen peroxide in elaborate electron-transfer chains for the reduction of molecular oxygen to water (18). When U23 cells were treated with diphenylene iodonium (DPI), an inhibitor of NADPH oxidase, 100 μM

for 2 h before the cytochrome c assay, superoxide production was decreased to ~50% of the original amount, and this difference was statistically significant (Fig. 2B, $p < 0.05$). However, when U23 cells were treated with 50 μM rotenone, an inhibitor of mitochondrial respiratory electron-transfer chains, for 2 h before

the cytochrome c assay, there was no change in the superoxide production. This suggested that superoxide was partially produced from an activated phagocyte-like NADPH oxidase system and not the mitochondria in the *v-Ha-ras* transfected cells. A possible mechanism consistent with earlier studies is that *v-Ha-ras* transduced cells express dominantly activated Ras, which activates downstream Rac, which in turn triggers NADPH activation (24); therefore, superoxide is produced. However, DPI is not totally specific as it inhibits other flavoproteins besides the NADPH oxidase; therefore, we cannot conclude for sure that the NADPH oxidase is involved, but it is a logical candidate.

MnSOD, CuZnSOD, and CAT protein levels were increased in v-Ha-ras transduced REC cells

During evolution, eukaryotic cells have developed a complex antioxidant enzyme system to protect against ROS. We demonstrated that *v-Ha-ras* transduced REC cells produced much more superoxide than parental cells; thus, we hypothesized that there may be some changes in the major antioxidant enzymes. To test this hypothesis, we used western blotting to examine the protein levels of different antioxidant enzymes. Western blotting demonstrated that MnSOD, CuZnSOD, and CAT immunoreactive protein levels were increased in W13, U12, and U23, compared with REC and Neo cells (Fig. 3A). We also performed native GPx immunoblotting; unfortunately, we did not obtain specific bands. Our results demonstrated that REC and Neo had low levels of superoxide radicals and antioxidant proteins, W13 had medium levels, and U12 and U23 had high levels.
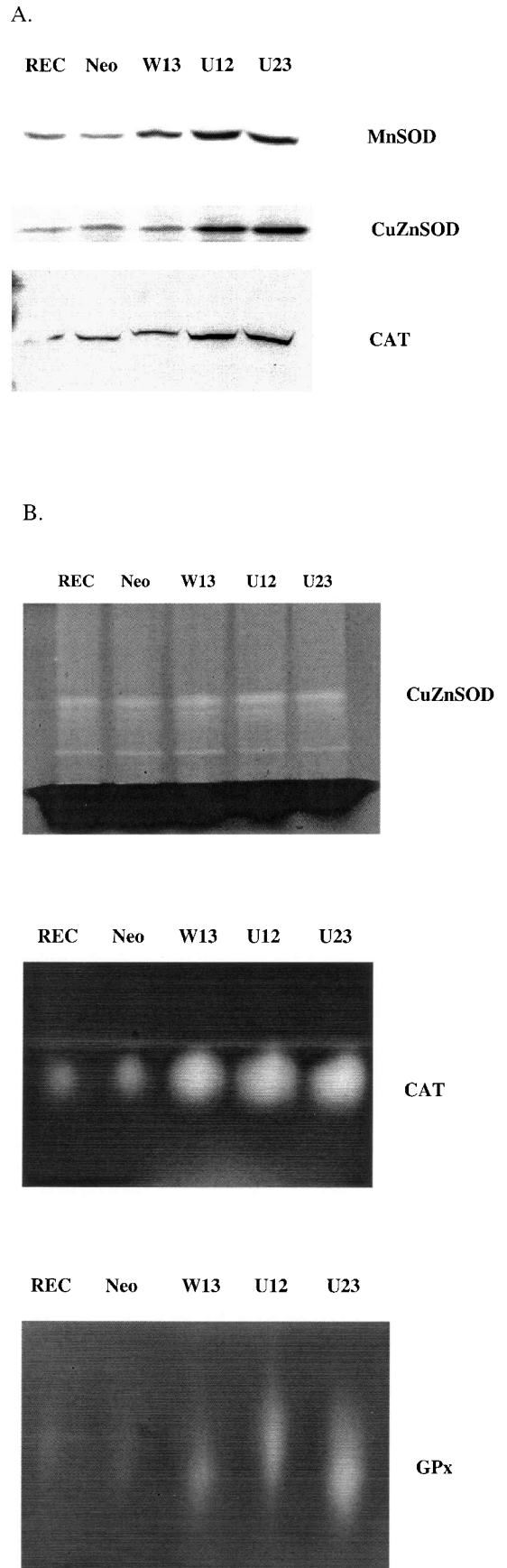

A.

REC Neo W13 U12 U23

MnSOD

CuZnSOD

CAT

B.

REC Neo W13 U12 U23

CuZnSOD

REC Neo W13 U12 U23

CAT

REC Neo W13 U12 U23

GPx

FIG. 3. **Changes of antioxidant enzyme levels in *v-Ha-ras* transduced REC cells.** (**A**) Western blotting for Mn-SOD, CuZnSOD, and CAT. Cell lysates (100 μg) were run on 12.5% SDS-PAGE, the proteins in gels were electro-transferred to nitrocellulose sheets, and the sheets were treated with anti-MnSOD, anti-CuZnSOD, or anti-CAT antibodies. Increased levels of immunoreactive protein for these antioxidant enzymes were found in Ras transduced cells. (**B**) Native activity gel assay for SOD, CAT, and GPx. Cell lysates (100 μg for SOD, 200 μg for CAT, and 400 μg for GPx) were used to run a native gel. The gels were stained; the achromatic bands showed the enzyme activities. Increased enzymatic activities for CuZn-SOD, CAT, and GPx were seen.

CuZnSOD, CAT, and GPx activities were increased in v-Ha-ras *transduced REC cells*

To test whether the primary antioxidant enzyme activities were also increased, we performed SOD, CAT, and GPx activity gel analysis; the results are shown in Fig. 3B. In the SOD activity gel, we first thought that the top band was MnSOD and the bottom band was CuZnSOD. However, we remembered that MnSOD from rat tissue is usually not visualized in these gels. We then examined the effect of cyanide on the activity of these bands. Cyanide inhibits CuZnSOD, but not MnSOD. We found that the top band was strongly inhibited and the bottom band was only inhibited a small amount. These results suggest that the top band is CuZnSOD, which increased with Ras levels. The identity of the bottom band is still unknown, but it is unlikely to represent MnSOD because the migration is too fast. Thus, we concluded that the activity of CuZnSOD was increased in Ras-overexpressing cell lines. The CAT and GPx activity gels also demonstrated that CAT and GPx activity increased in W13, U12, and U23 cells (Fig. 3B). Thus, the whole primary antioxidant enzyme system adjusted to the challenge of Ras-mediated superoxide production; the system members worked together to try to balance ROS in this new situation.

Cellular plating efficiency was increased and cell population doubling time was shortened in v-Ha-ras *transfected cells*

Ras transformation can promote the processes of carcinogenesis. Our results demonstrated that *v-Ha-ras* transfection induced superoxide production. We wanted to determine if there were any effects on cell clonogenic capability and cell growth. To determine the clonogenic ability of *v-Ha-ras* transduced cells, we performed a plating efficiency assay. We observed a significant increase in the plating efficiency of transfected cells compared with the parental cells (Fig. 4); U23 showed about a sevenfold increase, U12 demonstrated an approximately fivefold increase, and W13 had about a fourfold increase. This was a statistically significant observation with all three cell lines ($p < 0.05$). This demonstrates that *v-Ha-ras* transduced cells have increased clonogenic capability.

To determine the cell population doubling time, 2×10^4 cells were plated in 24-well plates; cells were counted every other day. Table 1 shows the cell population doubling time in hours. The doubling times for W13, U12, and U23 were 29.1, 24.4, and 24.8 h, respectively; for REC and Neo, the times were 39.3 and 35.4 h, respectively. Clearly, *v-Ha-ras* transduced cells had a shorter cell doubling time and proliferated faster.
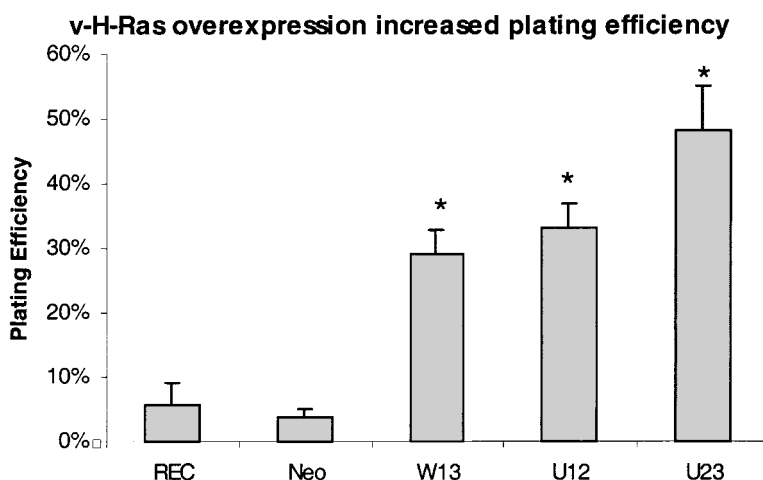

FIG. 4.   Plating efficiency was increased in *v-Ha-ras* **transduced REC cells.** Cells (100 or 500) were plated into 60-mm dishes and maintained in an incubator for 14 days to allow colony formation. The colonies were then fixed and stained with 0.1% crystal violet and 2.1% citric acid, and the colonies containing >50 cells were counted. Means were calculated from three experiments, and error bars represent SD. *Statistically significant difference from REC or Neo at the $p < 0.05$ level.

TABLE 1. v-Ha-Ras EXPRESSION SHORTENED CELL POPULATION DOUBLING TIME

Cells	REC	Neo	W13	U12	U23
Cell population doubling time (h)	39.3 ± 2.9	35.4 ± 4.8	29.1 ± 2.8	24.4 ± 2.3*	24.8 ± 1.9*

Cells (2×10^4) were plated in 1.5 ml of complete medium in 24-well plates. Cells were trypsinized and then counted on alternate days for 2 weeks using a hemocytometer, and cell population doubling time was calculated. Data are means ± SD.

*U12 and U23 are significantly different from REC or Neo ($p < 0.05$).

v-Ha-ras *transfection enhanced AP-1, AP-2, and NF-κB DNA binding*

The effects of *v-Ha-ras* transfection on transcription factor DNA-binding activity was investigated by electrophoretic gel mobility shift assays. AP-1, AP-2, and NF-κB DNA-binding activities were significantly increased in *v-Ha-ras* transduced cells compared with parental REC cells and vector controls. Fig. 5A shows that AP-1 DNA binding was greatly enhanced in the Ras transfectants W13, U12, and U23 when compared with that in parental and Neo cells. However, when U23 nuclear protein extracts were preincubated with 2 μg of anti-c-Jun/AP-1 antibody and then incubated with AP-1 ^{32}P-labeled probe, the DNA-binding activity was greatly inhibited (Fig. 5A, lane 6). The specificity of AP-1 binding to the DNA probe was further demonstrated by competition experiments with unlabeled oligos. The DNA–protein complex was partially or completely abolished in the presence of a 10- or 100-fold excess of unlabeled AP-1 probe (Fig. 5B, lanes 3 and 4), whereas 10- or 100-fold excess of unlabeled AP-2 and NF-κB oligos did not effectively compete for protein bound to the labeled AP-1 probe (Fig. 5B, lanes 5–8). These results demonstrate that the bands in W13, U12, and U23 lanes were due specifically to AP-1 DNA binding.

AP-2 DNA binding was also enhanced in W13, U12, and U23 cells compared with that in REC and Neo (Fig. 5C). The binding activity was supershifted when W13 nuclear protein extracts were preincubated with 2 μg of anti-AP-2α antibody (Fig. 5C, lane 6), which demonstrates that the bands in the W13, U12, and U23 lanes were due specifically to AP-2 DNA binding. Interestingly, AP-2 DNA-binding ac-

tivities appeared to decrease with increasing *v-Ha-ras* expression. NF-κB DNA-binding activity was also higher in W13, U12, and U23 (Fig. 5D), and supershift assays demonstrated that the binding was due specifically to the NF-κB–probe complex formation (Fig. 5D, lane 6). SP-1 was not activated in any of the cell lines studied (data not shown).

v-Ha-ras *transduction increased p44/p42 and p38 kinase activities*

In many cells, MAPK activation is dependent on the production of ROS after the stimulation of growth factors (7, 14, 15, 30). MAPKs in turn phosphorylate and activate certain transcription factors. We have demonstrated that DNA-binding activities of AP-1, AP-2, and NF-κB were increased in *v-Ha-ras* transduced REC cells. Therefore, we investigated whether certain MAPKs were turned on in these cells. We focused on these kinases, including p44/42, stress-activated protein kinase/JNK, and p38 MAPK, because they can phosphorylate and activate transcription factors. However, the activities of MAPKs are also dependent on their remaining in the phosphorylated form as only the phosphorylated kinases are active. Thus, their activities could be inferred by western blotting using antibodies against the phosphorylated form of these kinases. Fig. 6 suggests that p44/42 MAPK and p38 MAPK activities were increased in W13, U12, and U23, but not in REC and Neo cells, because both the phospho-p44/42 MAPK and phospho-p38 MAPK protein levels were increased in W13, U12, and U23 cells. Western blotting for phospho-JNK was also performed, but the result showed no difference in the protein level (data not shown). We cannot actually conclude in these studies
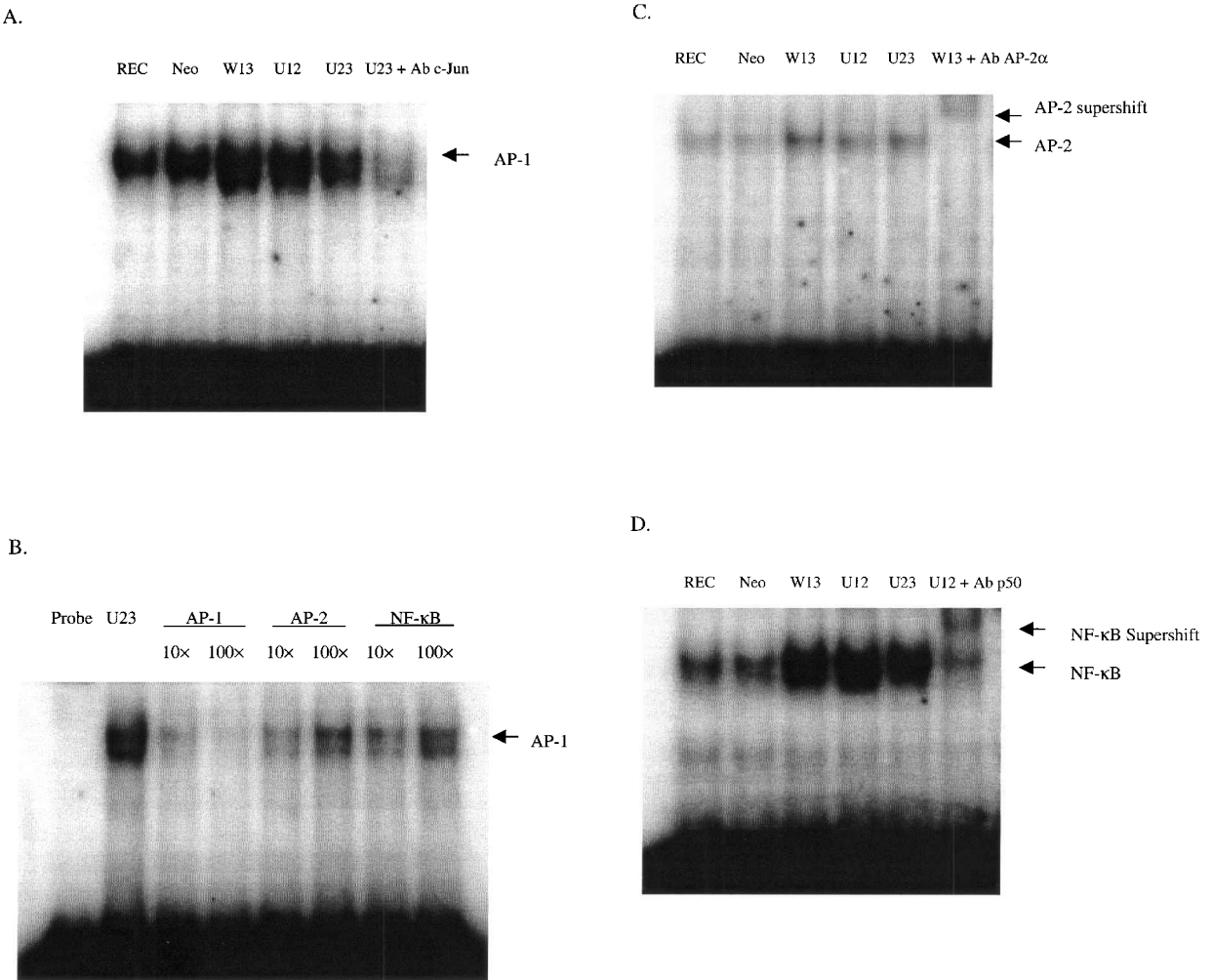
A.

B.

C.

D.

FIG. 5. **AP-1, AP-2, and NF-κB DNA-binding activities were increased in *v-Ha-ras* transduced REC cells.** (**A**) Ras transduction enhanced AP-1 DNA binding. Antibody against c-Jun/AP-1 was used for the antibody clearance experiment. (**B**) Specificity of AP-1 DNA binding. Oligonucleotides containing AP-1, AP-2, and NF-κB consensus sequences were used as competitors to demonstrate the specificity of AP-1 DNA binding to the AP-1 oligo. (**C**) Ras transduction enhanced AP-2 DNA binding. Antibody against AP-2α was used for supershift assay. (**D**) Ras transduction enhanced NF-κB DNA binding. Antibody against p50 was used for the supershift assay. Nuclear protein (1.5 μg) for each sample was incubated with ^{32}P-labeled oligo probes (for AP-1, AP-2, or NF-κB) in the presence of 1 μg of poly(dIdC) and 1× gel shift buffer at room temperature for 15 min. The binding reactions were loaded onto a 5% polyacrylamide gel and run at 35 mA for 45 min in 1× TBE buffer. The gels were wrapped in a sheet of plastic wrap and exposed to x-ray film overnight at −80°C.

that the kinases were activated because we did not measure the levels of total kinase protein. However, consistent with other studies, one possible mechanism is that superoxide production activated p44/42 MAPK and p38 MAPK; the kinases then phosphorylated and turned on AP-1, AP-2, and NF-κB. These transcription factors then induced a series of gene expressions, including possibly the induction of the antioxidant enzymes, that promote cell proliferation or inhibit cell death. Many of the

biological effects of *v-Ha-ras* can be accomplished by constitutive activation of these transcription factors.

DISCUSSION

ROS have been shown to play important roles in normal cell function; their balance in cells is controlled by the highly compartmentalized antioxidant enzyme system (20). We
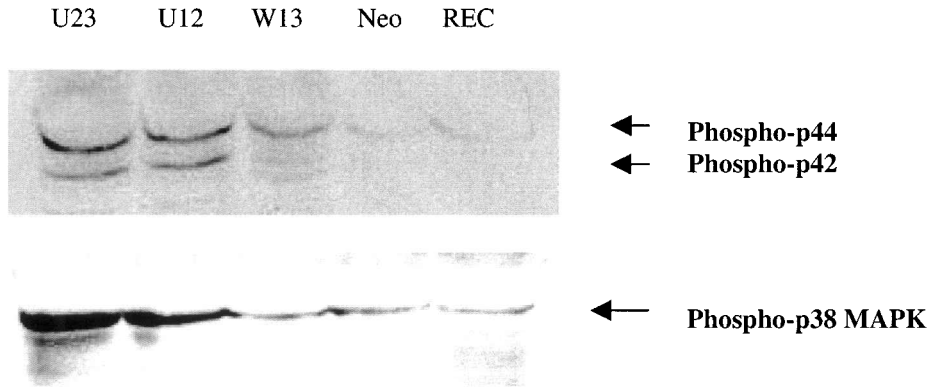
U23   U12   W13   Neo   REC

← Phospho-p44
← Phospho-p42

← Phospho-p38 MAPK

FIG. 6.   The protein levels of phospho-p44/p42 and phospho-p38 MAPK were increased in the *Ras*-transduced REC cells. Cell lysates (200 μg) were used to run on 12.5% SDS-PAGE; then the proteins in gels were electrotransferred to nitrocellulose sheets, and the sheets treated with anti-phospho-p44/p42 MAPK or anti-phospho-p38 MAPK antibodies. Western blotting demonstrated that both phospho-ERK and phospho-p38 MAPK protein levels were increased. Coomassie Blue staining of transferred gel indicated equal protein loading.

have demonstrated that *v-Ha-ras* mediated superoxide production in Ras transfected REC cells. Moreover, Ras overexpression also modulated antioxidant enzyme levels, increased DNA-binding activity of transcription factors AP-1, AP-2, and NF-κB, and increased protein levels of phosphorylated MAPK p44/p42, and p38 in these cells. The transfected cells possessed typical Ras phenotypes, including shortened cell doubling time and increased cellular plating efficiency. These results suggest that Ras mitogenic signaling may be mediated partly though redox regulation by superoxide.

Oncogenic *ras* can transform many immortal cell lines to the tumorigenic state and plays a central role in cellular signal transduction. There are at least two possible signaling pathways for Ras to pass mitogenic signaling; one is the well defined Ras–Raf pathway, and another is the Ras–Rac–superoxide pathway. In the second pathway, Ras activates Rac, which can promote the NADPH oxidase to generate superoxide; superoxide can activate MAPKs and transcription factors to induce mitogenic effects. Previous work has shown that Ras can mediate superoxide overproduction. When fibroblasts were transformed by mutant oncogenic Ras, superoxide production was detected in the transformed cells, but not in parental and vector control cells, and the Ras-transformed cells displayed a greater rate of DNA synthesis (11). Dr. Bar-Sagi's research suggests that

Rac-induced superoxide production is a critical mediator of mitogenic signaling (12). This evidence suggests that Ras proteins could induce mitogenic signaling partially through modification of the superoxide production in these cells.

Our studies have demonstrated for the first time that *v-Ha-ras* transduced REC cells increased primary antioxidant enzyme levels, including MnSOD and CuZnSOD levels. However, cancer cells generally express low, constitutive levels of MnSOD and CuZnSOD when compared with their cells of origin (19, 20). One possible reason for this discrepancy in antioxidant proteins is that cancer development is a long and multiple-step process; during this process, MnSOD and CuZnSOD gene transcription becomes less active than their cells of origin. We have found that DNA methylation in the MnSOD promoter region could inhibit transcription factor binding (10), which provides one mechanism to explain this phenomenon. Although the cell line we used in the present studies is immortal, it is still in an early stage of the carcinogenic process (less than 30th passage), and thus, the primary antioxidant enzyme genes could still show normal transcription activity. Another paradox is that increased SOD activity has usually been shown to slow cell proliferation in either normal or malignant cells (13, 20); in the present work, increased SOD is associated with increased cell prolifer-

ation. One possible explanation for this is that the cells with higher SOD activity may be protected against cell death due to apoptosis or necrosis.

Approximately 30% of all human tumors have *ras* mutations, which implies that increased superoxide may be produced in these cells. However, cancer cells usually have less MnSOD and CuZnSOD activity; this suggests that cancer cells may take advantage of superoxide overproduction to promote cell proliferation. As less superoxide is scavenged by MnSOD or CuZnSOD, tumor cells can maintain a relatively higher steady-state level of superoxide, which may act as a mediator of mitogenic signaling. In the present study, it appeared that the hydrogen peroxide-scavenging enzymes were increased more by Ras overexpression than the superoxide-scavenging enzymes. This would suggest that Ras overexpression might lead to larger increases in superoxide radical than hydrogen peroxide. Studies of the effects of modulating superoxide production on Ras mitogenic signaling will provide insights into the mechanisms linking superoxide and growth control.

ACKNOWLEDGMENTS

ABBREVIATIONS

AP-1 and AP-2, activator protein-1 and -2; CAT, catalase; CuZnSOD, copper- and zinc-containing superoxide dismutase; DPI, diphenylene iodonium; GPx, glutathione peroxidase; JNK, c-jun N-terminal kinase; MAPK, mitogen-activated protein kinase; MnSOD, manganese-containing superoxide dismutase; NF-κB, nuclear factor-κB; α-PA, α-hydroxyfarnesylphosphonic acid; PAGE, polyacrylamide gel electrophoresis; Ras, Ras protein; *ras*, *ras* gene or mRNA; REC, rat kidney epithelial cell; ROS, reactive oxygen species; SD, standard deviation; SDS, sodium dodecyl sulfate; SOD, superoxide dismutase; SSC, saline–sodium citrate buffer; TBE, Tris–borate–EDTA.

REFERENCES

1. Beauchamp C and Fridovich I. Superoxide dismutase: improved assays and an assay applicable to acrylamide gels. *Anal Biochem* 44: 276–287, 1971.

2. Butler J, Koppenol WH, and Margoliash E. Kinetics and mechanism of the reduction of ferricytochrome *c* by the superoxide anion. *J Biol Chem* 257: 10747–10750, 1982.

3. Cepko CL, Roberts BE, and Mulligan RC. Construction and applications of a highly transmissible murine retrovirus shuttle vector. *Cell* 37: 1053–1062, 1984.

4. Cotran RS, Kumar V, and Robbins SL. *Pathologic Basic of Disease*, 5th edit. Philadelphia, PA: W.B. Saunders Company, 1994.

5. Freeman BA. Biological sites and mechanisms of free radical production. In: *Free Radicals in Molecular Biology, Aging, and Disease*, edited by Armstrong D, Sohal RS, Cutler RG, and Slater TF. New York, Raven Press, 1984, pp. 43–52.

6. Fridovich I. Cytochrome *c*. In: *CRC Handbook of Methods for Oxygen Radical Research*, edited by Greenwald RA. Boca Raton, FL: CRC Press, Inc., 1985, pp. 121–122.

7. Guyton KZ, Liu Y, Gorospe M, Xu Q, and Holbrook N. Activation of mitogen-activated protein kinase by H_2O_2. Role in cell survival following oxidant injury. *J Biol Chem* 271: 4138–4142, 1996.

8. Henderson LM and Chappell JB. NADPH oxidase of neutrophils. *Biochim Biophys Acta* 1273: 87–107, 1996.

9. Huang Y and Domann FE. Redox modulation of AP-2 DNA binding activity in vitro. *Biochem Biophys Res Commun* 249: 307–312, 1998.

10. Huang Y, Peng J, Oberley LW, and Domann FE. Transcriptional inhibition of manganese superoxide dismutase (SOD2) gene expression by DNA methylation of 5′ CpG island. *Free Radic Biol. Med* 23: 314–320, 1997.

11. Irani K, Xia Y, Zweier JL, Sollott SJ, Der CJ, Fearon ER, Sundaresan M, Finkel T, and Goldschmidt-Clermont PJ. Mitogenic signaling mediated by oxidants in Ras-transformed fibroblasts. *Science* 275: 1649–1652, 1997.

12. Joneson T and Bar-Sagi D. A Rac1 effector site controlling mitogenesis through superoxide production. *J Biol Chem* 273: 17991–17994, 1998.

13. Lam E, Zwacka R, Engelhardt JF, Davidson BL, Domann FE, Yan T, and Oberley LW. Adenovirus-mediated manganese superoxide dismutase gene transfer to hamster cheek pouch carcinoma cells. *Cancer Res* 57: 5550–5556, 1997.

14. Levine A, Tenhaken R, Dixon R, and Lamb C. H_2O_2 from the oxidative burst orchestrates the plant hypersensitive disease resistance response. *Cell* 79: 583–593, 1994.

15. Liu Y, Guyton KZ, Gorospe M, Xu Q, Lee J, and Holbrook N. Differential activation of ERK, JNK/SAPK and p38/CSBP/RK MAP kinase family members during the cellular response to arsenite. *Free Radic Biol Med* 21: 771–781, 1996.

16. Lowy DR and Willumsen BM. Function and regulation of ras. *Annu Rev Biochem* 62: 851–891, 1993.
17. Muller JM, Cahill MA, Rupec RA, Baeuerle PA, and Nordheim A. Antioxidants as well as oxidants activate c-fos via Ras-dependent activation of extracellular-signal-regulated kinase 2 and Elk-1. *Eur J Biochem* 244: 45–52, 1997.
18. Nohl H and Jordan W. The mitochondrial site of superoxide formation. *Biochem Biophys Res Commun* 138: 533–539, 1986.
19. Oberley LW and Buettner GR. Role of superoxide dismutase in cancer: a review. *Cancer Res* 39: 1131–1149, 1979.
20. Oberley LW and Oberley TD. Role of antioxidant enzymes in the cancer phenotype. In: *Oxygen, Gene Expression and Cellular Function*, edited by Clerch L and Massaro D. New York, NY: Marcel Dekker Inc., 1997, pp. 279–307.
21. Oberley TD, Oberley LW, Slattery AF, Lauchner LJ, and Elwell JH Immunohistochemical location of antioxidant enzymes in adult Syrian hamster tissues and during kidney development. *Am J Pathol* 137: 199–214, 1990.
22. Pagano PJ, Clark JK, Cifuentes-Pagano ME, Clark SM, Callis GM, and Quinn MT. Localization of a constitutively active phagocyte-like NADPH oxidase in rabbit aortic adventitia: enhancement by angiotensin II. *Proc Natl Acad Sci U S A* 94: 14483–14488, 1997.
23. Pai EF, Kabsch W, Krengel U, Holmes KC, John J, and Wittinghofer A. Structure of the guanine-nucleotide-binding domain of the Ha-ras oncogene product p21 in the triphosphate conformation. *Nature* 341: 209–214, 1989.
24. Prigmore E, Ahmed S, Best A, Kozma R, Manser E, Segal AW, and Lim L. A 68-kDa kinase and NADPH oxidase component p67phox are targets for Cdc42Hs and Rac1 in neutrophils. *J Biol Chem* 270: 10717–10722, 1995.
25. Pulverer BJ, Kyriakis JM, Avruch J, Nikolakaki E, and Woodgett JR. Phosphorylation of c-jun mediated by MAP kinases. *Nature* 353: 670–674, 1991.
26. Santillo M, Mondola P, Gioielli A, Seru R, Iossa S, Annella T, Vitale M, and Bifulco M. Inhibitors of Ras farnesylation revert the increased resistance to oxidative stress in K-Ras transformed NIH 3T3 cells. *Biochem Biophys Res Commun* 229: 739–745, 1996.
27. Sen CK and Packer L. Antioxidant and redox regulation of gene transcription. *FASEB J* 414: 709–720, 1996.
28. Sun Y, Elwell JH, and Oberley LW. A simultaneous visualization of the antioxidant enzymes glutathione peroxidase and catalase on polyacrylamide gels. *Free Radic Res Commun* 5: 67–75, 1988.
29. Sundaresan M, Yu ZX, Ferrans VJ, Irani K, and Finkel T. Requirement for generation of H_2O_2 for platelet-derived growth factor signal transduction. *Science* 270: 296–299, 1995.
30. Sundaresan M, Yu Z, Ferrans VJ, Sulciner DJ, Gutkind JS, Irani K, Goldschmidt-Clermont PJ, and Finkel T. Regulation of reactive-oxygen-species generation in fibroblasts by Rac1. *Biochem J* 318: 379–382, 1996.
31. Turner CP, Toye AM, and Jones OTG. Keratinocyte superoxide generation. *Free Radic Biol Med* 24: 401–407, 1997.
32. Yang J-Q, Li J, Domann FE, Buettner GR, and Oberley LW. Superoxide generation in v-Ha-*ras*-transduced human keratinocyte HaCaT cells. *Mol Carcinog* 26: 180–199, 1999.

Address reprint requests to:
Dr. Larry W. Oberley
Free Radical and Radiation Biology Program
B180 Medical Laboratories
Department of Radiology
The University of Iowa
Iowa City, IA 52242-1181

E-mail: larry-oberley@uiowa.edu